

## Supplementary Information

### Chemical Heterogeneity in Interfacial Layers of Polymer Nanocomposites

Siyang Yang,<sup>a</sup> Siqi Liu,<sup>a</sup> Suresh Narayanan,<sup>b</sup> Chongfeng Zhang,<sup>a</sup> and Pinar Akcora<sup>\*a</sup>

<sup>a</sup> Department of Chemical Engineering & Materials Science, Stevens Institute of Technology, Hoboken, NJ 07030, USA

<sup>b</sup> Advanced Photon Source, Argonne National Laboratory, Argonne, IL 60439, USA

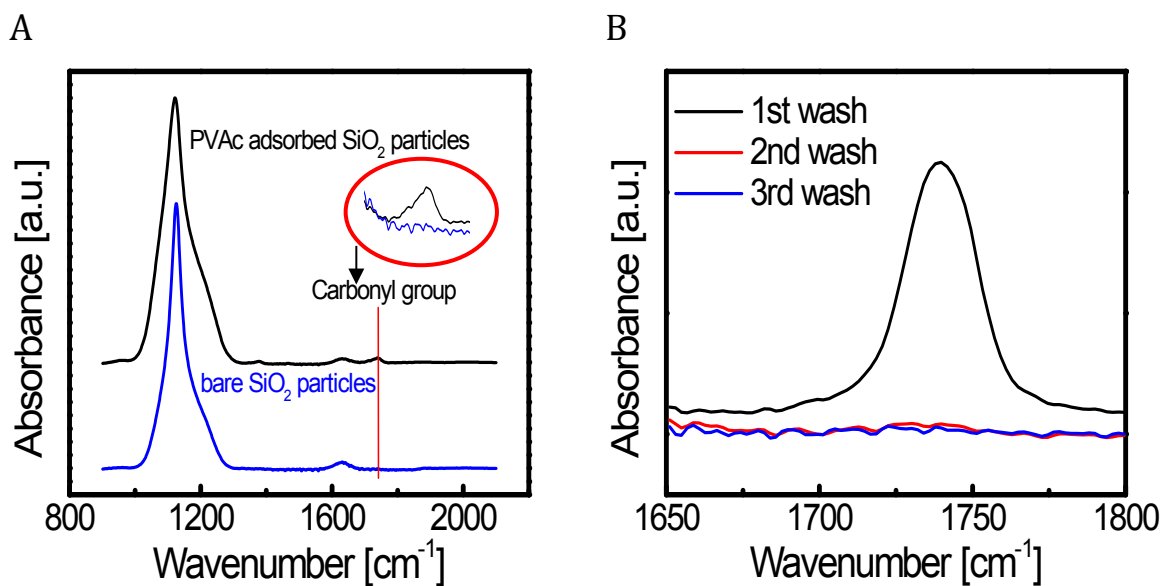


**Fig. S1 (A)** Absorbance peak of carbonyl group at 1740 cm<sup>-1</sup> indicates that PVAc is adsorbed on SiO<sub>2</sub> nanoparticles that are solvent-washed three times. Inset shows enlarged region of the carbonyl peak. **(B)** FTIR spectra of the supernatant after washing particles in dichlorobenzene and centrifuging.

The adsorbed and matrix polymers are varied as discussed in the manuscript to study the effects of  $T_g$  differences and miscibility of chains with different chemistries on mechanical properties of nanocomposites. The good dispersion of nanoparticles in PMA and PEO composites is not surprising and supports our discussion on the reinforcement effect observed with the adsorbed chain lengths.

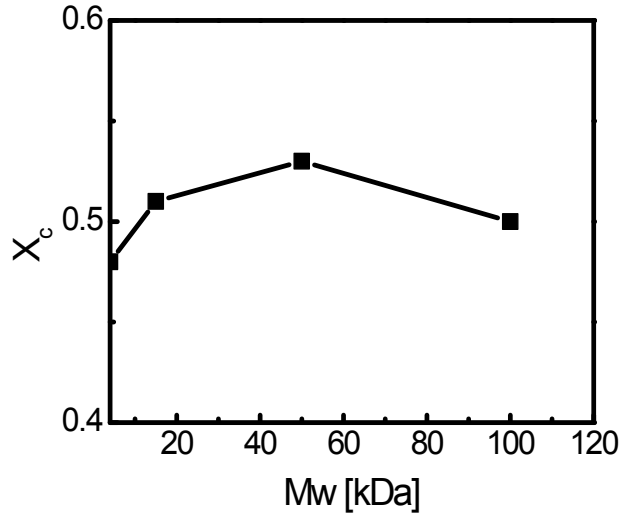


**Fig. S2** Degree of crystallinity ( $X_c$ ) remains relatively unchanged in PEO composites with different adsorbed PVAc chain lengths on particles. Particle loading is 30wt% in all samples.

The XRD patterns of composites with adsorbed PVAc chains with different molecular weights show almost identical crystalline peak positions of PEO at  $18.5^\circ$  from the crystal plane (120);  $22.5^\circ$  from the crystal plane (112); and  $26.0^\circ$  from the crystal plane (033). The peaks are used for determining the parameters of unit cell structure. For a monoclinic system, the inter-planar spacing of the (hkl) reflection planes is given by

$$\frac{1}{d^2} = \frac{1}{\sin^2 \beta} \left( \frac{h^2}{a^2} + \frac{k^2 \sin^2 \beta}{b^2} + \frac{l^2}{c^2} - \frac{2hl \cos \beta}{ac} \right)$$

where the value of  $\beta$  is  $125.4^\circ$ . The unit cell parameters and spacings are listed in Table S1. The monoclinic crystal structures for different composites suggest the adsorbed chains length does not influence the size of PEO unit cells.

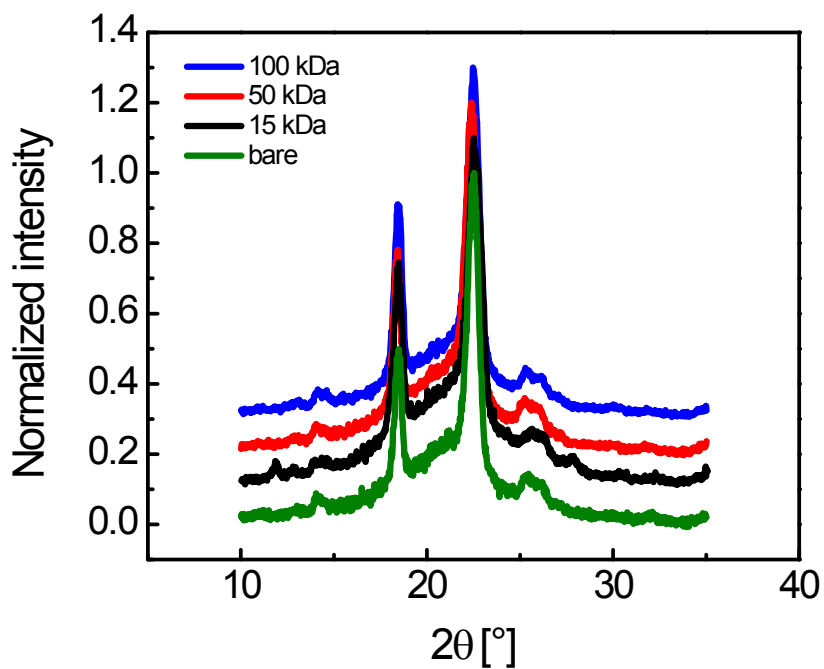


**Fig. S3** XRD patterns of PEO composites with bare and PVAc adsorbed SiO<sub>2</sub> at 30wt%. Data is shown for different molecular weights of adsorbed PVAc. Intensity was normalized with the peak intensity at 2θ of 22.5° and the baselines were shifted vertically.

**Table S1** Unit cell structure and crystalline parameters of bare and PVAc adsorbed particles in PEO (unit: Å)

Monoclinic	a	b	c	d(120)	d(033)	d(112)
bare	8.20	13.68	19.83	4.78	3.48	3.94
15 kDa PVAc adsorbed	8.30	13.56	19.67	4.79	3.45	3.95
50 kDa PVAc adsorbed	8.21	13.81	19.87	4.81	3.50	3.95
100 kDa PVAc adsorbed	8.17	13.75	19.89	4.79	3.50	3.94

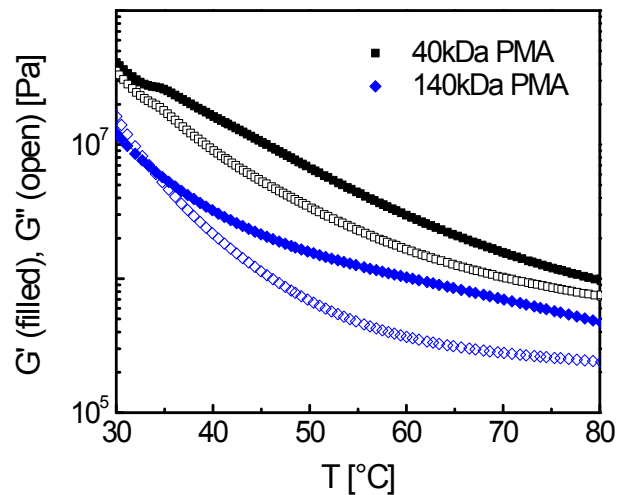


**Fig. S4** Elastic and viscous moduli of PMA (40 kDa, 140 kDa) nanocomposites with 50 kDa PVAc adsorbed SiO<sub>2</sub> as a function of temperature.

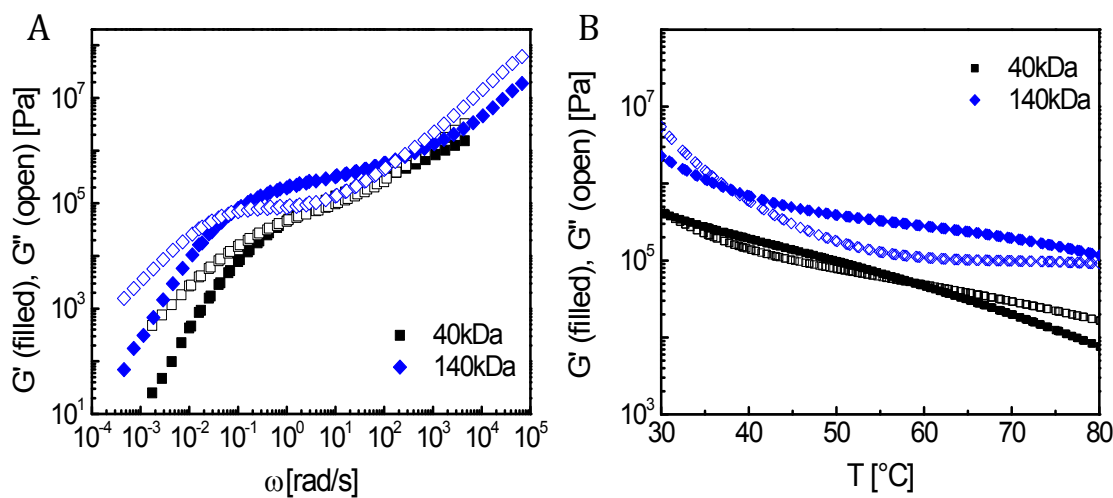


**Fig. S5 (A)** TTS master curves 40 kDa and 140 kDa PMA homopolymer **(B)** storage and loss moduli of 40 kDa and 140 kDa PMA homopolymer as a function of temperature.

### Effect of Adsorbed Chain Length in PMA composites

Time-temperature superposition of frequency data shows relaxations at an extended frequency range for bare and PVAc-adsorbed silica in 40 kDa PMA matrix at 30 wt% particle loading (Figure S6). The reinforcement effect and broadening of the rubbery plateau is clearly observed with the longer adsorbed

chains. This reinforcement is attributed to the polar interactions between the two polymers. The subsequent dynamic coupling decreases the mobility of matrix chains, thereby enhances the mechanical properties of nanocomposites. Plateau modulus at low frequency indicates a network formation with the longer (100 kDa) adsorbed chains. The crossover of elastic and viscous moduli is at lower frequency for bare composites than for PVAc-adsorbed composites and the rubber-liquid transition of bare particles appears at a higher frequency (**Fig. 5A**). This indicates that some dynamic coupling between PVAc and PMA may be leading to faster glass-rubber relaxations. At low frequencies, the mobile PVAc and PMA chains are highly entangled acting as physical constraints to deformation. The slow dynamics of PVAc adsorbed chains led to slowing of the PMA matrix dynamics at the interface. The minimum loss tangent ( $\tan\delta$ : the ratio of viscous modulus to elastic modulus) of 30 wt% PVAc adsorbed nanocomposites appeared at 45°C, which was at the lower temperature than that of bare-PMA composite. The confinement effect imposed by the glassy PVAc chains lowered the glass-rubbery transition (Fig. S6), but this effect was not prominent due to the small  $T_g$  difference between PVAc and PMA. These results indicate that having chemical heterogeneity in the interphase can improve the bulk viscoelastic properties, particularly with the appropriate selection of polymers which may chemically interact. SEM images of freeze-fractured nanocomposites show good dispersion in 40 kDa PMA matrix with the bare and PVAc adsorbed silica particles (Fig. S8).

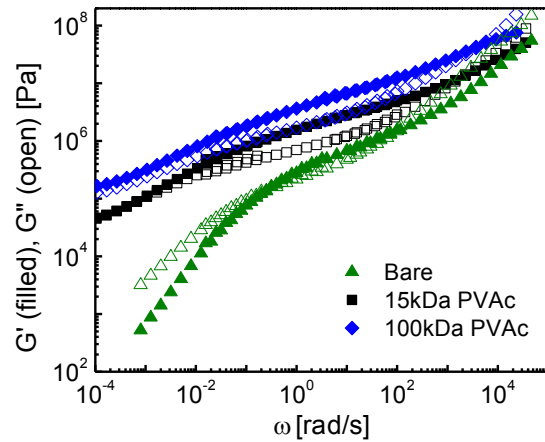


**Fig. S6** Effect of adsorbed chain length on the viscoelastic properties of PMA (40 kDa) composites with 30 wt% loading. TTS master curves of 15 kDa and 100 kDa adsorbed PVAc and with bare nanoparticles in 40 kDa PMA at a reference temperature of 55°C.

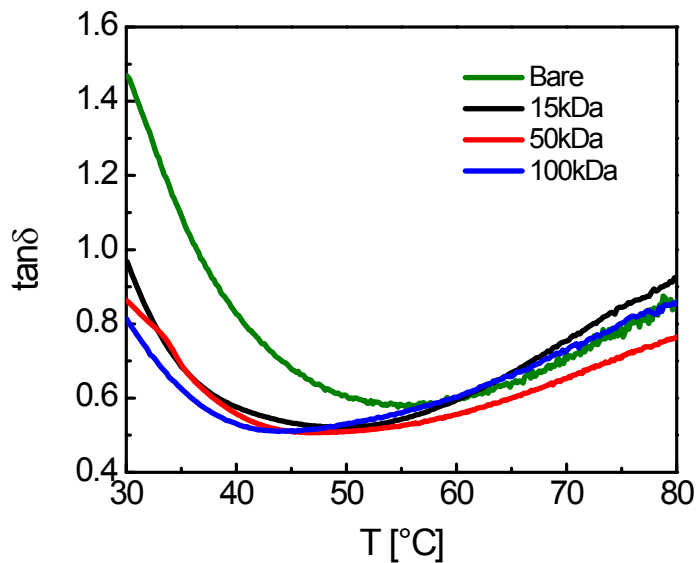


**Fig. S7** Loss tangent ( $\tan\delta$ ) of 40 kDa PMA nanocomposites with 15, 50, 100 kDa PVAc adsorbed particles as a function of temperature at a frequency of 5 rad/s, and at the strain amplitudes in linear viscoelastic regime. Particle loading is 30 wt% in all.

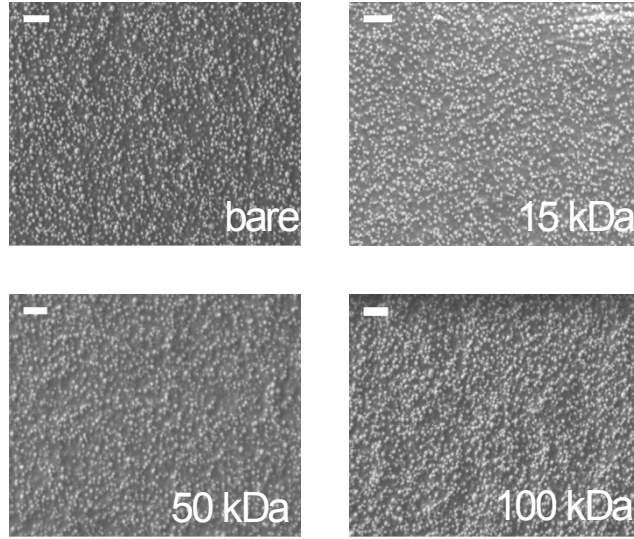


**Fig. S8** SEM images of 15 kDa, 50 kDa, and 100 kDa PVAc adsorbed and bare SiO<sub>2</sub> in 40 kDa PMA matrix with 30 wt% loading. Scale bar is 500 nm.

The scattering data in Figs. 1 and 4 were modelled by using the following equations. The scattering

intensity,  $I(q)$ , is described by 
$$I(q) = \int_0^{\infty} n(r)P(q)S(q)dr$$
.  $n(r)$  is the particle size distribution function,  $P(q)$  is the form factor, and  $S(q)$  is the structure factor for Percus-Yevick hard sphere model<sup>1,2</sup>.  $n(r)$  is described

by a Gaussian distribution: 
$$n(r) = \frac{1}{\sigma\sqrt{2\pi}} e^{-\frac{1}{2}\left(\frac{r-r_0}{\sigma}\right)^2}$$
, where  $r_0$  is the mean radius,  $\sigma$  is the standard deviation. A unified sphere form factor,  $P(q)$ , was described as<sup>3</sup>:

$$P(q) = \exp\left(-\frac{q^2 R_g^2}{3}\right) + B \left[ \frac{\left(\text{erf}\left(\frac{q R_g}{\sqrt{6}}\right)\right)^3}{q} \right]^4$$

where  $R_g = \sqrt{\frac{3}{5}} r_0$ ,  $B = \frac{1.62}{R_g^4}$ .

1. S. R. Kline, *J. Appl. Crystallogr.*, 2006, **39**, 895-900.
2. J. K. Percus and G. J. Yevick, *Physical Review*, 1958, **110**, 1.
3. G. Beaucage, *J. Appl. Crystallogr.*, 1995, **28**, 717-728.

